

V. PERVAK^{1,✉}
A.V. TIKHONRAVOV²
M.K. TRUBETSKOV²
S. NAUMOV¹
F. KRAUSZ^{1,3}
A. APOLONSKI^{3,4}

1.5-octave chirped mirror for pulse compression down to sub-3 fs

¹ Max-Planck-Institut für Quantenoptik, Hans-Kopfermann-Str. 1, 85748 Garching, Germany
² Research Computing Center, Moscow State University, Leninskie Gory, 119992 Moscow, Russia
³ Ludwig-Maximilians-Universität München, Am Coulombwall 1, 85748 Garching, Germany
⁴ Institute of Automation and Electrometry, RAS, 630090 Novosibirsk, Russia

Received: 22 August 2006/Revised version: 6 September 2006
Published online: 18 October 2006 • © Springer-Verlag 2006

ABSTRACT We demonstrate numerically and experimentally a chirped mirror with controlled reflectivity and dispersion of up to 1.5 octaves. A complementary pair of such mirrors has a reflectivity of 95% in the wavelength range 400–1200 nm with residual group delay dispersion ripples $< 100 \text{ fs}^2$ in all of this range. The mirror pair allows one to compensate a chirp of the corresponding spectrum (with a smooth phase), resulting in sub-3-fs pulses.

PACS 42.65.Re; 42.79.Fm; 42.79.Wc

1 Introduction

Generation of one-cycle pulses has been a challenge in optics for decades. Such pulses are indispensable for studying extremely short processes in gas, liquid and solid-state media; one example is the study of dephasing processes in water. There are two main approaches to generating one-cycle pulses: (i) synthesis of different laser sources [1–3] or a Raman generator on the basis of synthesis of vibrational or rotational transitions in molecules [4–6] with further pulse compression by means of a spatial light modulator (SLM) [4], and (ii) compression of a supercontinuum behind hollow gas-filled fibers [7–9]. The shortest visible 3.4-fs pulses so far have been obtained in experiments with supercontinuum generation in hollow gas-filled fibers [7, 9] combined with a SLM. Further progress in these two approaches is limited by both the low transmission of a SLM and the highest pulse energy that can be applied to the SLM.

An alternative to a SLM can be a broadband chirped mirror (CM) compressor. There has been progress in chirped mirror development since its invention in 1994 [10]. All previous efforts have been concentrated on design and realization of CMs approaching one octave [11–16], but generation of one-cycle, ~ 2.5 -fs pulses at the central wavelength of 800 nm already entails manipulation with a 1.5-octave spectrum, for which the phase must be corrected. In this paper we demonstrate the feasibility of designing such broadband CMs in terms of theory and simulations and show their first realizations.

2 Theory and design

A CM is a dispersive optical interference coating usually designed by optimizing the initial multilayer design. A CM is characterized by a certain value of the group delay dispersion (GDD), the second derivative of the phase shift on reflection with respect to the angular frequency. A CM can provide the broadband spectrum with support, comparable with prism and grating pairs, but additionally it offers control of third- and higher-order dispersions and higher efficiency (reflectivity) together with better beam stability. Reflection from the top layer of a multilayer structure brings so-called ripples to the spectral GDD curve due to interference between waves reflected from the top layer and waves which have penetrated and been reflected from deeper. Ripples become pronounced in the case where air is an incident medium. In general, the mirror GDD should compensate the material (through which the initially short pulse passes) or the (nonlinear) pulse chirp so that the residual dispersion fluctuations are acceptably small in all of the relevant spectral range. Usually, during design optimization, residual fluctuations drop to a low level. The GDD fluctuations can broaden the pulse and lead to energy transfer from the initial single pulse to satellites. The period of the ripples in the spectral domain determines the position of the satellite in the temporal domain, and the amplitude of these oscillations determines the amount of energy which transfers into the satellite(s).

A bandwidth of a CM and its GDD spectral shape are defined by, among other parameters, impedance mismatch between the ambient medium and mirror stack. The impedance mismatch can be overcome by using glass as the medium of incidence. Unfortunately, this solution limits the highest value of GDD, because the mirror stack should compensate an additional thin non-parallel substrate [17] or glass wedge [18]. Additionally, in this case the aperture cannot be high and the beam stability problem may arise. There are several other approaches to reducing GDD ripples: double-chirped mirrors [19], Brewster-angled CMs [20] and complementary CM pairs [11]. Alternatively, time-domain optimization [13, 21] deals directly with pulse compression and can therefore lead to the shortest pulses even in spite of large GDD oscillations. The complementary mirror approach has high potential and the relevant results are shown below.

✉ Fax: +49-089-289-14141, E-mail: volodymyr.pervak@mpq.mpg.de

For providing pulse compression down to sub-3 fs, it is necessary to design a complementary CM pair with smooth dispersion and high reflectivity in all of a 1.5-octave spanning spectrum. Note that the requirement of dispersion smoothness is greater for a broader spectrum. An appropriate design of such an ultra-broad CM (UBCM) is a complex thin-film problem requiring fast optimization algorithms and a powerful computer to calculate a large number of target points.

In this work the OptiLayer software was used for designing the mirror. The distinguishing feature of OptiLayer is its completely analytical approach to computing all quantities necessary for coating optimization [22]. This feature provides a computational efficiency that cannot be achieved when non-analytical approaches are applied to coating optimization. It is recalled that the characteristic GDD to be optimized is the second derivative of the phase shift with respect to the angular frequency, and modern highly efficient optimization methods also require second derivatives of this characteristic with respect to layer thicknesses. Utilizing the completely analytical approach to computing all derivatives required provides fast computation and high accuracy of the synthesis algorithms at all stages of designing.

In order to design a complementary CM pair a special plug-in module was developed. We define the target reflectance of a CM pair reduced to a single mirror as

$$R_p = (R_1 R_2)^{1/2}, \quad (1)$$

and the target GDD as

$$\text{GDD}_p = (\text{GDD}_1 + \text{GDD}_2) / 2, \quad (2)$$

where the subscript p designates values relating to a CM pair and the subscripts 1, 2 designate a mirror in the pair. It is convenient to operate with values reduced to a single mirror in order to simplify comparison of the obtained characteristics

with the single-mirror case. By means of (1) and (2) we define the merit function

$$F = \frac{1}{L} \sum_{j=1}^L \left(\frac{R_p(\lambda_j) - R^{(j)}}{\Delta R^{(j)}} \right)^2 + \left(\frac{\text{GDD}_p(\lambda_j) - \text{GDD}^{(j)}}{\Delta \text{GDD}^{(j)}} \right)^2, \quad (3)$$

where $R_p(\lambda_j)$ and $\text{GDD}_p(\lambda_j)$ are theoretical characteristics at wavelength λ_j , $R^{(j)}$ and $\text{GDD}^{(j)}$ are target values, $\Delta R^{(j)}$ and $\Delta \text{GDD}^{(j)}$ are corresponding tolerances and L is the number of selected wavelength points. In order to perform synthesis of CM pairs, needle optimization [23] and gradual evolution [24] techniques were generalized to the case of the merit function (3). In particular, the adapted needle optimization algorithm seeks all possible positions for new layer insertions in both mirrors.

Two different designs in which the GDD curves have the same oscillations and are shifted only by half of their period can be used as initial designs for further optimizing the average dispersion. For a pair of CMs covering less than one octave, such a design can be easily realized.

We designed two pairs of UBCMs. The one pair (UBCM1 and UBCM2) was optimized by using the GDD target, while the other pair (UBCM3 and UBCM4) was designed by using the group delay (GD) target. The GDD target for the optimization program corresponds to an ideal design with 100% reflection in a desirable bandwidth together with the GDD curve necessary to exactly compensate a certain amount of material. The GD target is defined in a similar way and can be optimized by means of the merit function (3) with obvious substitution of GD for GDD. Below we describe the advantage and disadvantage of each target approach.

The design of the UBCM1,2 pair demonstrates high residual ripples (Fig. 1) because the initial design periods of the GDD oscillations have been chosen different. The average curve has high ripples in the middle of the spectral range

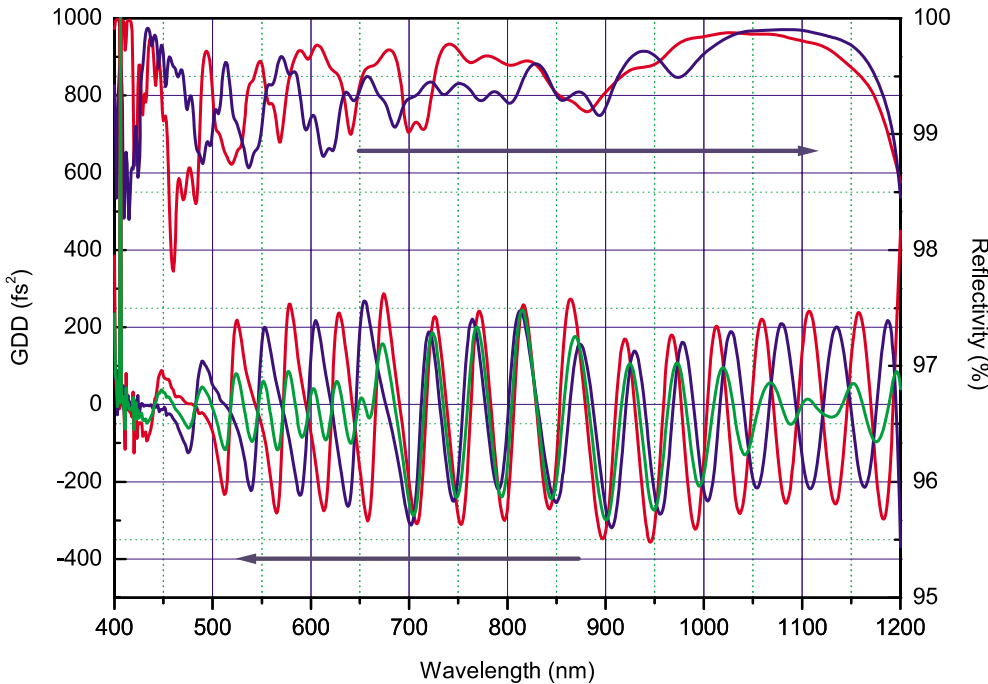


FIGURE 1 Calculated reflectivity and GDD of UBCM1 and UBCM2. Red: UBCM1; blue: UBCM2. The green curve is an averaged GDD of UBCM1 and UBCM2 per bounce

around 800 nm and smaller ripples in the wings. The amplitude of the ripples of each design is tolerable, $\pm 200 \text{ fs}^2$, but the average dispersion curve oscillates around the target value.

The layer thickness structures of the designs are shown in Fig. 2a and b. The physical layer thicknesses are between 5 nm and 193 nm. The layers with thicknesses 5–25 nm are very sensitive to errors during the deposition procedure, and the relative thickness error is greater for a thin layer. In order to decrease the sensitivity of a CM design to thickness errors, we applied a de-sensitization procedure (which is a part of the OptiLayer software [25]) based on the following idea [26].

Let us introduce a penalty function characterizing the sensitivity of a mirror to small errors in layer thickness. Keeping the main linear terms in variation of the merit function (3) with respect to layer thickness variations, one obtains

$$P = \sum_{ij} \left(\frac{1}{\Delta R^{(j)}} \frac{\partial R_{1,2}(\lambda_j)}{\partial d_i} \right)^2 + \sum_{ij} \left(\frac{1}{\Delta \text{GDD}^{(j)}} \frac{\partial \text{GDD}_{1,2}(\lambda_j)}{\partial d_i} \right)^2. \quad (4)$$

Small values of the penalty function P correspond to low sensitivity of mirror 1 or 2 to thickness errors, while large values correspond to high sensitivity. Thus, we can consider a new optimization problem with the objective function

$$\Phi = F + \alpha P \quad (5)$$

and control parameter α . Varying parameter α , one can control the influence of the penalty function P in the course of optimization of the objective function Φ (5). Low values of the control parameter α provide low penalty values and the

solution of the optimization problem with the objective function (5) will be close to the solution of the initial problem with the merit function (3). High values of α usually cause large variations of layer thickness and a significant increase of the first term F in (5), which means a significant degradation of the spectral performance of the mirror. There exists a so-called ‘golden middle’ value of the control parameter α providing a decrease of sensitivity without noticeable degradation of the spectral performance. We selected the golden middle value interactively in the course of solving the optimization problem (5).

The results of this procedure are shown in Fig. 2c and d. Before the procedure nearly all sensitive layers were situated among the last (top) layers, whereas after it they were redistributed more homogeneously.

The UBCM1,2 pair provides negative GDD of around -35 fs^2 at 800 nm and high reflectivity in the wavelength range 400–1200 nm. According to the design, one mirror bounce roughly compensates 1 mm of fused silica. This spectral range corresponds to sub-3-fs pulses for the smooth phase. However, a time-domain analysis shows (see below) that this mirror pair cannot compress pulses down to sub-3-fs duration, the reason being unacceptably high residual dispersion ripples.

The second pair UBCM3,4 consists of 78 and 80 layers. There are also many thin layers, shown in Fig. 3a and b. This pair provides a negative GDD of -20 fs^2 at 800 nm. The mirror design was chosen to compensate the dispersion of 3 m of air and 3 mm of fused silica for 10 bounces. The reflectivity and the GD curves of this pair are shown in Fig. 4. For the UBCM3,4 pair we avoided the inconsistency in the periods, which was present for UBCM1,2. Sharp thin spikes in both the

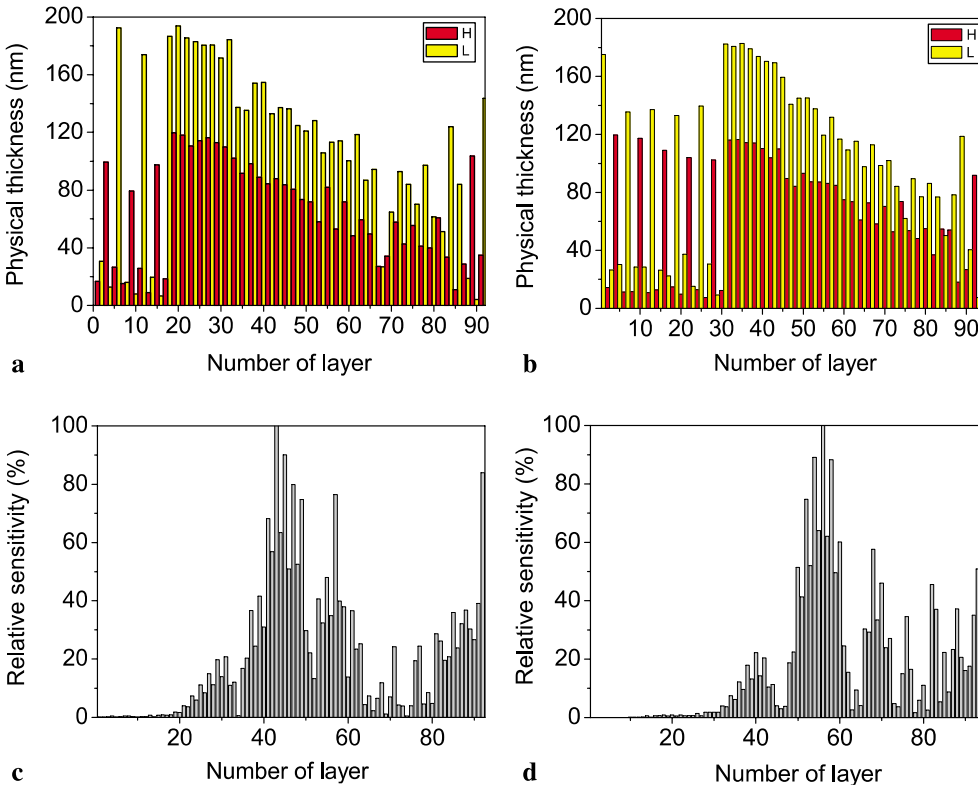


FIGURE 2 Design of the UBCM1 (a) and UBCM2 (b) thickness profiles. The red and yellow colors denote materials with high refractive index and low refractive index, respectively. Number of layers: 92 and 95, respectively. The relative sensitivity of the layers to errors after de-sensitization: UBCM1 (c) and UBCM2 (d)

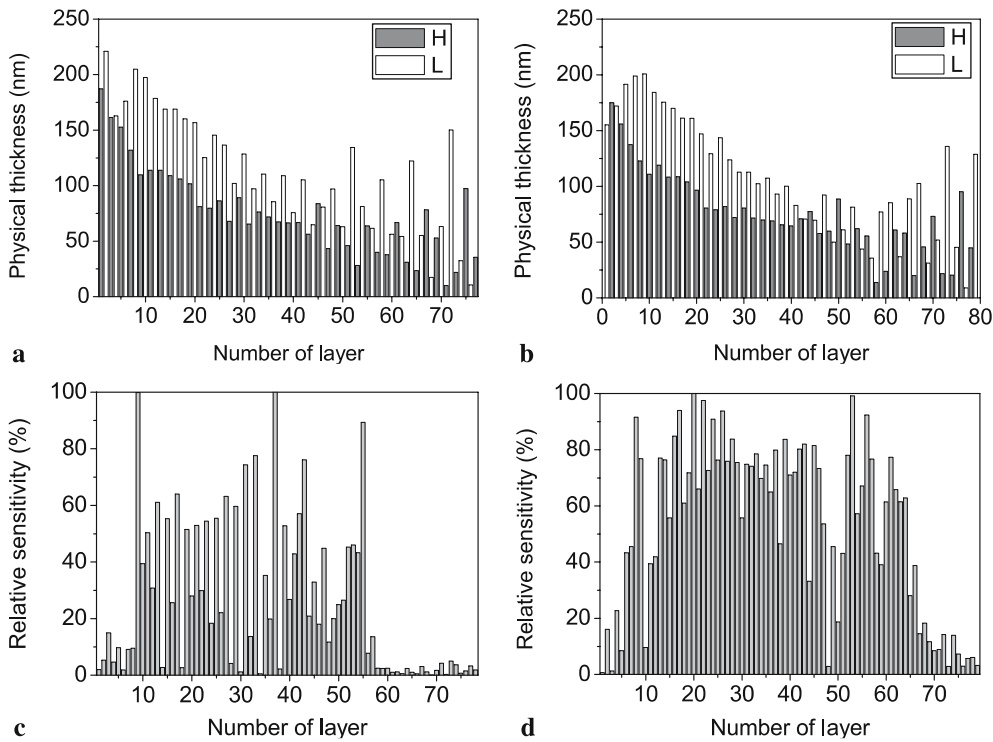


FIGURE 3 Design of the UBCM3 (a) and UBCM4 (b) thickness profiles. The red and yellow colors denote materials with high refractive index and low refractive index, respectively. The relative sensitivity of the layers to errors after de-sensitization: UBCM3 (c) and UBCM4 (d)

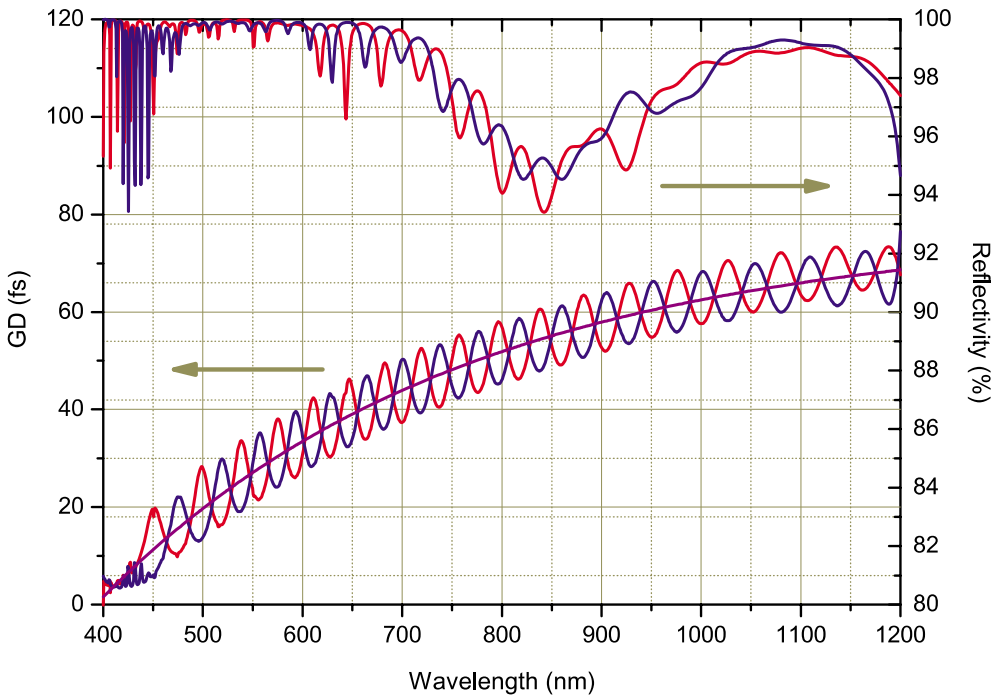


FIGURE 4 Calculated reflectivity and group delay (GD) of UBCM3 and UBCM4. The red curves show UBCM3, the blue curves UBCM4. The violet curve is the target group delay for UBCM3 and UBCM4 per bounce

reflection and the GDD curves are clearly seen in the range 400–450 nm in Figs. 4 and 5. The appearance of sharp spikes is typical of ultra-broadband reflectors, but theoretical discussion thereof would exceed the scope of this publication. Suffice it to mention here that this phenomenon is associated with resonance effects inside a high-reflection multilayer structure at certain wavelengths [27]. The typical width of the GDD spikes for the UBCM3,4 pair is smaller than 0.3 nm. We found numerically that these spikes do not lead to satellites in the time domain, contrary to the ripples.

The design of the UBCM3,4 pair is similar to the design of the UBCM1,2 pair: all the layers sensitive to error are concentrated among the top layers of the designs. The relative sensitivity became more uniform after the de-sensitization procedure, as shown in Fig. 3c and d.

Figure 6 shows how the UBCM chirped mirror works. The electric field components at 1200 nm penetrate much deeper into the multilayer structure than the components at 400 nm. This means that the infrared components become delayed relatively to the blue ones. Figure 6 gives an additional hint

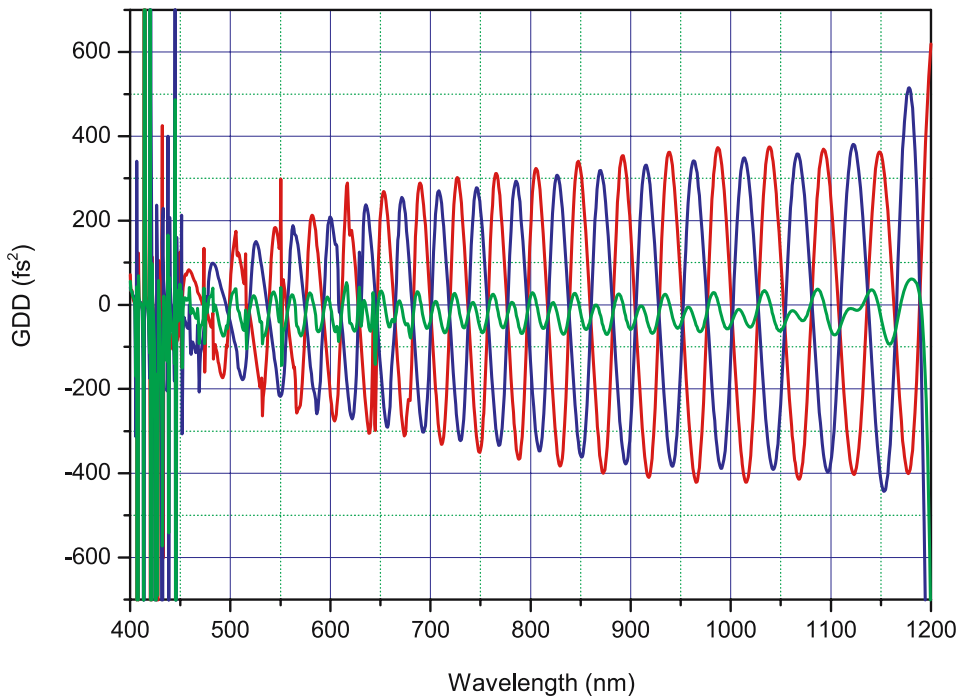


FIGURE 5 Calculated GDD of UBCM3 and UBCM4. The *red curve* corresponds to UBCM3, the *blue curve* to UBCM4. The *green curve* is the average GDD of UBCM3 and UBCM4 per bounce

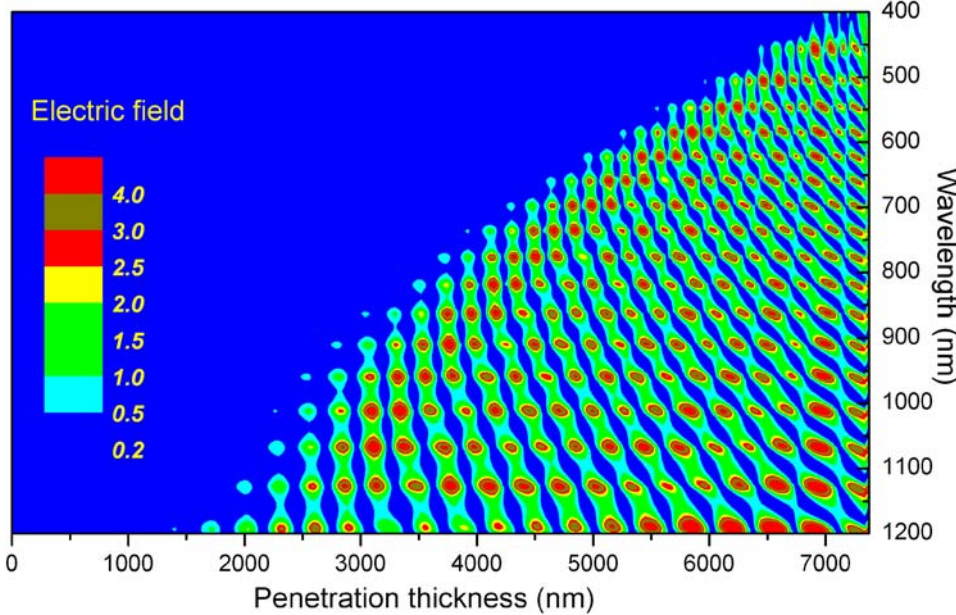


FIGURE 6 Penetration of electric field through the multilayer structure of UBCM3

for optimizing the design: the long-wavelength components must penetrate almost down to the first layer. If this is not the case in the design, several layers must be removed. In the opposite case, viz. when long-wavelength components penetrate through the entire multilayer structure including the substrate, several layers must be added. This only applies to mirrors with negative dispersion.

We estimated the total amount of GDD needed for a real compression experiment to be -200 fs^2 at 800 nm. Bearing in mind the GDD value -20 fs^2 for one bounce from UBCM3,4, we have to prove that 10 bounces of these mirrors do not destroy the incident pulse in terms of its duration and energy.

Figure 7 shows the combined results of temporal pulse analysis of the pulse reflected after several bounces of the

UBCM1,2 and UBCM3,4 pairs. In the analysis the main part of the dispersion was taken away and only residual GDD ripples were included.

We used a Gaussian free-chirp incident pulse centered at 800 nm (spectrum 400–1200 nm) with the spectrum corresponding to a bandwidth-limited pulse (FWHM) 2.48 fs. The reflected pulse does not become longer when the ripples are small or absent. For the UBCM1,2 pair, the reflected pulse duration grows to 4.13 fs after one bounce. After three bounces, the energy in the main pulse is only 10% of the initial value. This means that this pair of mirrors cannot be used for the proposed compression experiment. Nevertheless, this pair shows that production of a 1.5-octave CM with small dispersion ripples is possible for (i) the standard simple single-chirped stack

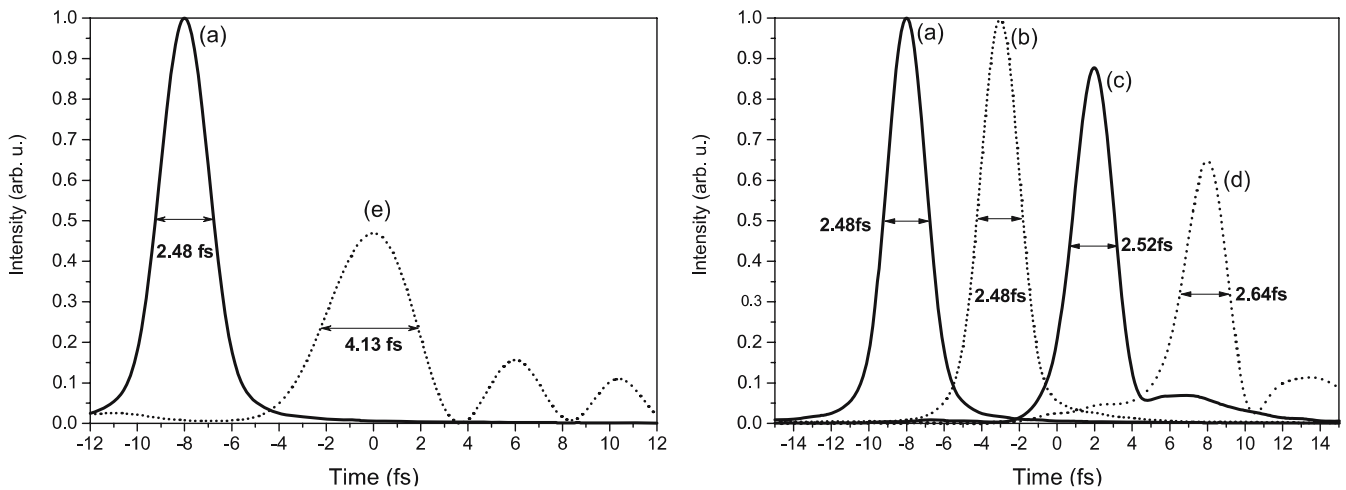


FIGURE 7 Temporal analysis of the reflection of an incident Gaussian-shaped free-chirp 2.48-fs pulse (a) from the UBCM1,2 pair (left) and UBCM3,4 pair (right). The curve (e) corresponds to the envelope of the pulse reflected from the UBCM1,2 pair after one bounce, (b) after one bounce from the UBCM3,4 pair, (c) after five bounces from the UBCM3,4 pair and (d) after 10 bounces from the UBCM3,4 pair. The temporal shift of the curves is artificial

and (ii) the complementary pair approach. Calculations for the UBCM3,4 pair demonstrate that after 10 bounces (i) the incident pulse extends only up to 2.64 fs and (ii) the energy losses of the pulse are 50%. This value can be considered as acceptable at this initial stage of research and bearing in mind $\sim 15\%$ of the SLM throughput [6].

The reason for such different performance of the two pairs of UBCMs is that the average GDD spectral curve fluctuates around the target curve and has comparably high ripples in the case of UBCM1,2. Our estimations supported by numerical simulations (Fig. 7) show that the residual GDD ripples must be smaller than $\pm 50 \text{ fs}^2$ to provide satisfactory operation. As was mentioned above, the residual GDD ripples can be of higher amplitude without affecting the pulse if time-domain optimization is applied [13, 21].

3 Experiment

The UBCM mirrors were produced with the magnetron-sputtering Helios machine (Leybold Optics). Helios is equipped with two proprietary TwinMags magnetrons and a plasma source for plasma/ion-assisted reactive middle-frequency dual-magnetron sputtering. The magnetrons were optimized for high sputtering rates and high optical layer performance. The system was pumped by turbo-molecular pumps to 1×10^{-6} mbar before deposition. Argon and oxygen were used for both magnetrons. In the magnetron cathodes, Nb and Si targets were used. The electric power of the Si cathode is 4500 W and the power of the Nb cathode is 3500 W. The power applied to the Nb cathode was not constant because it operated in the oxygen control (or lambda control) mode, which guaranteed stable film properties. The gas pressure was 1×10^{-3} mbar during the sputtering process. Oxygen was fed near the targets to oxidize the sputtering films. The distance from the targets to the substrates was 100 mm. The purity of the Si target was 99.999% and that of the Nb target 99.9%. By changing the electric power applied to the cathode, it was possible to increase or decrease the sputtering rate. We found that the film quality degrades at high rates and good film quality was realized at a rate of around 0.5 nm/s

for both materials. In the experiments we used BK7 and FS substrates.

The transmission spectra were measured with a Perkin-Elmer spectrophotometer (Lambda 950). The GDD was determined by using a white-light interferometer (WLI) with a spectral accuracy of 5 nm and the dispersion accuracy $\sim 10 \text{ fs}^2$. The current version of the WLI operates only in the range 400–1100 nm.

The sensitivity of the designs was very high, so that even the layer thickness error of 0.5% led to unsatisfactory results. Two control techniques were tested to provide a high production accuracy of the layers: time control and optical control. We chose the time control technique because optical control failed for such complex designs: there are many thin layers of thicknesses 5–20 nm that cannot be controlled with optical control.

We chose Nb_2O_5 (refractive index is 2.35 at 500 nm) as high-refraction-index material. Other materials are unsuitable: TiO_2 has high losses in the range below 500 nm, whereas Ta_2O_5 and HfO_2 have lower refractive indices leading to relatively narrowband performance. SiO_2 was chosen as a material with low refractive index. Its refractive index is 1.48 at 500 nm. The measured values of the refractive indices are higher than those determined by evaporation techniques. The $\text{Nb}_2\text{O}_5/\text{SiO}_2$ pair already recommended itself in our experiments with the one-octave CM [11] due to (i) low losses for the broadband wavelength range 400–1200 nm and (ii) the highest difference in the refractive indices.

Due to high deposition rates, it took only six hours to produce one CM, even for complex chirped multilayer structures. We found that the actual refractive index of the layers must be determined just before the manufacturing process starts and then the initial design has to be finally re-optimized with the new refractive-index values. The values of the refractive index and physical thickness of a film are necessary for the time control technique. To determine the refractive index and the physical thickness of a single layer, we measured its transmission spectral curve and then used the OptiChar module from the OptiLayer software package [25]. During the characterization we determined the spectral dependence of the refractive index

using the three-parameter Cauchy model and assumed that the films have no absorption in the working spectral range. There are certain experimental difficulties in determining the refractive index n and the physical film thickness d separately from the measurements. The method of determining the optical properties of a thin film by transmission measurement is not very precise, but fast enough. The accuracy of this method is about 0.5% and sufficient for our application.

Spectral measurements of UBCM1,2 and UBCM 3,4 show very good agreement with the design in respect of both reflectivity and dispersion; see Figs. 8–10. If the calculated and measured GDD curves are close to each other, the errors made during deposition are small or it is the result of

effective error compensation. Compensation means here that a smaller refractive index can be compensated by a greater physical thickness of the layer, thus keeping the optical thickness constant. In the case of the CM, compensation works when the errors in determining the refractive index or the layer thickness are smaller than 1%.

It should be mentioned that the data presented in Figs. 8–10 contain two different spectral measurements of GD and GDD: the one between 400 and 610 nm and the other between 600 and 1100 nm. Accordingly, there can be small disagreements in these ranges, e.g. in the relative amplitudes of the GD and GDD oscillations. The very good agreement between the design and measurements in the range 400–1100 nm leads us

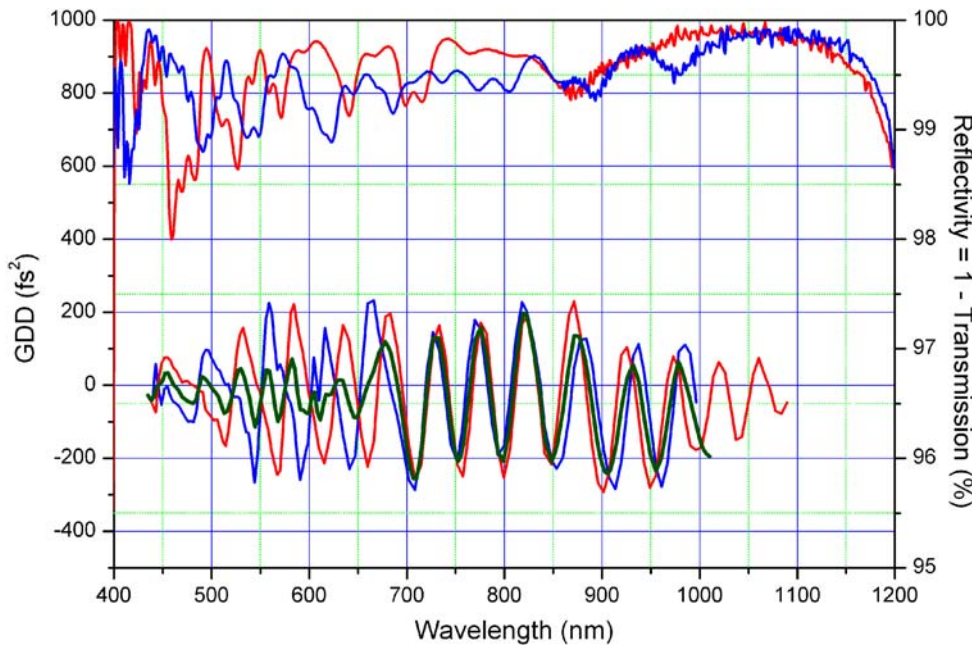


FIGURE 8 Measured reflectivity (obtained from the transmission data) and group delay dispersion of UBCM1 and UBCM2. The red curves correspond to UBCM1, the blue curves to UBCM2. The green curve is the average group delay dispersion of UBCM1 and UBCM2 per bounce

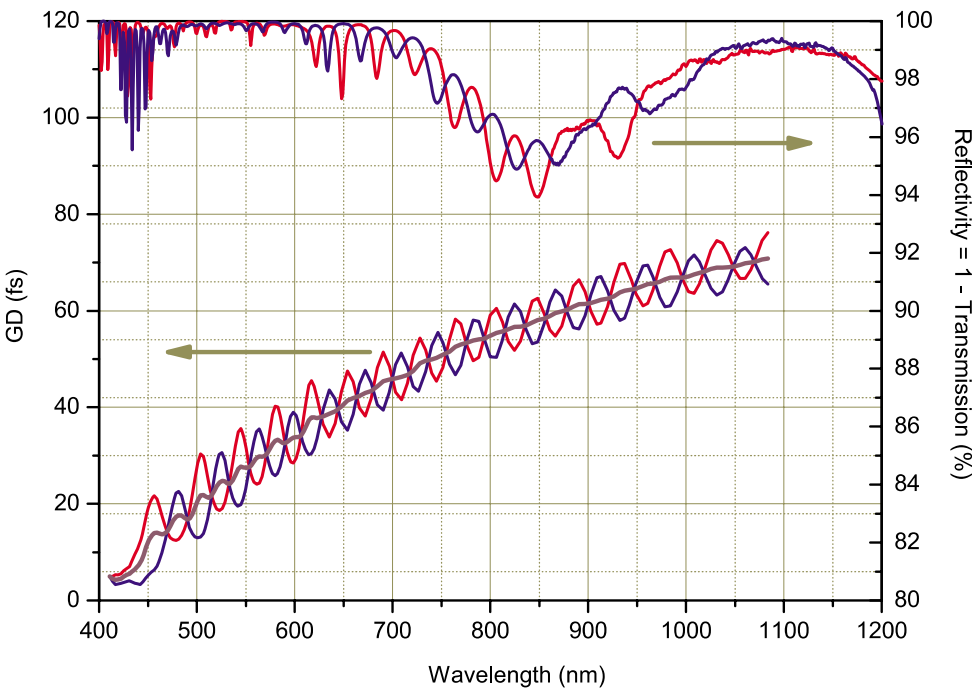


FIGURE 9 Measured reflectivity (obtained from the transmission data) and group delay of UBCM3 and UBCM4. The red curves correspond to UBCM3, the blue curves to UBCM4. The violet curve is the average group delay of UBCM3 and UBCM4 per bounce

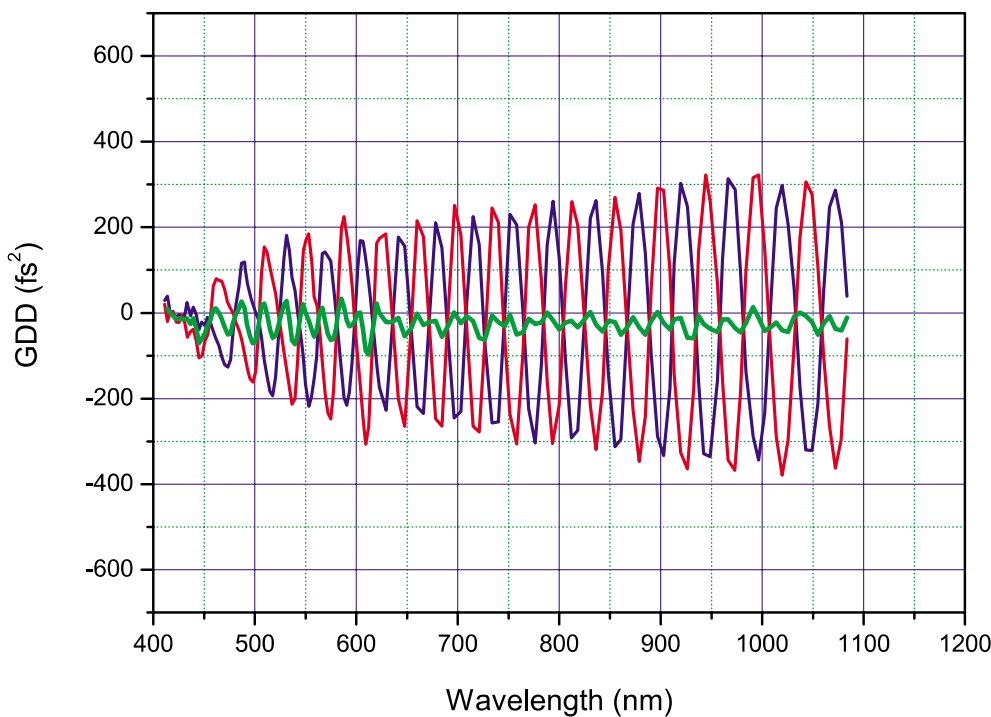


FIGURE 10 Measured GDD of UBCM3 and UBCM4. The red curve corresponds to UBCM3, the blue curve to UBCM4. The green curve is the average group delay dispersion of UBCM3 and UBCM4 per bounce

to assume that the GDD curve behaves in a predictable way in the range 1100–1200 nm as well.

4 Conclusions

We have proposed two different approaches to design an ultra-broad CM. In the case of the GDD target approach, the main disadvantage is that the average value of the dispersion fluctuates around the target value. In the time domain this means that a reasonable amount of energy transfers from the pulse into the satellites after one bounce. By using the GD as a target for optimization, one can avoid fluctuations of the average value of GDD. As a result, the reflected pulse is only 6% broader than the incident one even after 10 bounces and contains ~ 50% of the initial energy.

For the first time, we have demonstrated both the design and realization of an ultra-broad CM capable of compressing optical pulses down to sub-3 fs in the spectral range 400–1200 nm. We believe that this approach is still not at its limit. Another material combination with higher refractive-index contrast and better accuracy of deposition together with further development of the mathematical approaches to the design procedure could push the now existing 1.5-octave frontier toward two octaves.

ACKNOWLEDGEMENTS The authors are grateful to V. Yakovlev for valuable discussions and support with the time-domain pulse calculations.

REFERENCES

- O. Albert, G. Mourou, *Appl. Phys. B* **69**, 207 (1999)
- T.W. Hänsch, *Opt. Commun.* **80**, 71 (1990)
- Y. Kobayashi, H. Takada, M. Kakehata, K. Torizuka, *Appl. Phys. Lett.* **83**, 839 (2003)
- M.Y. Shverdin, D.R. Walker, D.D. Yavuz, G.Y. Yin, S.E. Harris, *Phys. Rev. Lett.* **94**, 033904 (2005)
- M. Spanner, M.Y. Ivanov, *Opt. Lett.* **28**, 576 (2003)
- N. Zhavoronkov, G. Korn, *Phys. Rev. Lett.* **88**, 203901 (2002)
- M. Nisoli, S. De Silvestri, O. Svelto, R. Szipöcs, K. Ferencz, C. Spielmann, S. Sartania, F. Krausz, *Opt. Lett.* **22**, 522 (1997)
- G. Steinmeyer, G. Stibenz, *Appl. Phys. B* **82**, 175 (2006)
- K. Yamane, Z. Zhang, K. Oka, R. Morita, M. Yamashita, A. Suguro, *Opt. Lett.* **28**, 2258 (2003)
- R. Szipöcs, K. Ferencz, C. Spielmann, F. Krausz, *Opt. Lett.* **19**, 201 (1994)
- V. Pervak, S. Naumov, G. Tempea, V. Yakovlev, F. Krausz, A. Apolonski, *Proc. SPIE* **5963**, 490 (2005)
- G. Steinmeyer, *Appl. Opt.* **45**, 1484 (2006)
- P. Dombi, V.S. Yakovlev, K. O’Keeffe, T. Fuji, M. Lezius, G. Tempea, *Opt. Express* **13**, 10888 (2005)
- V. Yakovlev, G. Tempea, *Appl. Opt.* **41**, 6514 (2002)
- F.X. Kärtner, U. Morgner, R. Ell, T. Schibli, J.G. Fujimoto, E.P. Ippen, V. Scheuer, G. Angelow, T. Tschudi, *J. Opt. Soc. Am. B* **18**, 882 (2001)
- V.S. Yakovlev, P. Dombi, G. Tempea, C. Lemell, J. Burgdörfer, T. Udem, A. Apolonski, *Appl. Phys. B* **76**, 329 (2003)
- N. Matuschek, L. Gallmann, D.H. Sutter, G. Steinmeyer, U. Keller, *Appl. Phys. B* **71**, 509 (2000)
- G. Tempea, V. Yakovlev, B. Bacovic, F. Krausz, K. Ferencz, *J. Opt. Soc. Am. B* **18**, 1747 (2001)
- F.X. Kärtner, N. Matuschek, T. Schibli, U. Keller, H.A. Haus, C. Heine, R. Morf, V. Scheuer, M. Tilsch, T. Tschudi, *Opt. Lett.* **22**, 831 (1997)
- G. Steinmeyer, *Opt. Express* **11**, 2385 (2003)
- G. Tempea, V. Yakovlev, F. Krausz, *Interference coatings for ultrafast optics*. In *Optical Interference Coatings*, ed. by N. Kaiser, H. Pulker (Springer, Berlin Heidelberg, 2003)
- A.N. Tikhonov, A.V. Tikhonravov, M.K. Trubetskov, *Comput. Math. Math. Phys.* **33**, 1339 (1993)
- A.V. Tikhonravov, M.K. Trubetskov, G.W. DeBell, *Appl. Opt.* **35**, 5493 (1996)
- A.V. Tikhonravov, M.K. Trubetskov, T.V. Amotchkina, M.A. Kokarev, *Proc. SPIE* **5250**, 312 (2004)
- OptiLayer software: <http://www.optilayer.com>
- A.V. Tikhonravov, M.K. Trubetskov, T.V. Amotchkina, A.A. Tikhonravov, *Proc. SPIE* **4829**, 1061 (2003)
- A.V. Tikhonravov, D.Sc. thesis, Physics Faculty, Moscow State University (1986)